

The impact of ocean coupling on the track simulation of Typhoon Nanmadol (2022)

Akiyoshi Wada

Meteorological Research Institute, Tsukuba, Ibaraki, 305-0052, JAPAN

awada@mri-jma.go.jp

1. Introduction

A tropical depression became Typhoon Nanmadol near the Ogasawara Islands at 18 UTC on 13 September 2022. Nanmadol then rapidly deepened its central pressure from 00 UTC on 15 September, reaching 910 hPa at 18 UTC on 16 September. Although it turned to weaken rapidly north of 28°N from 15 UTC on 17 September, its central pressure was 940 hPa at landfall around Kagoshima. Heavy rainfall was observed around the Kyushu region due to the long duration of developing rain clouds, which may be associated with the track of the typhoon. We conducted numerical simulations on Nanmadol from the early developing phase to the decaying phase using the Japan Meteorological Agency nonhydrostatic atmosphere model (NHM) and the atmosphere-wave-ocean coupled model (CPL: Wada et al., 2018) under different atmospheric conditions at an initial integration time. The simulation results were used to assess the effect of ocean coupling on the track of Nanmadol and the rapid decaying north of 28°N.

2. Experimental design

The following computational domain is the same in all the NHM and CPL experiments. The domain is 4920 km (zonal) x 4740 km (meridional) of which center location is 34.0°N, 140°E. The horizontal resolution is 3 km. The number of vertical layers is 55 (the top height is about 27 km). The time step for the atmosphere model is 10s, that for the ocean model is 60s and that for the ocean surface wave model is 360s. All the simulations are started from 18UTC on 14 September in 2022. The integration period is 105 hours.

An initial condition and 6-hourly boundary conditions for the atmosphere are created from the global objective atmospheric analysis data of the Japan Meteorological Agency (~20 km horizontal resolution). In addition, an initial condition for the ocean is created from the North Pacific version of the oceanic analysis data (~0.1° horizontal resolution) merged with the Optimally Interpolated SST (OISST) daily product (0.25° horizontal resolution) obtained from the Remote Sensing Systems (<http://www.remss.com>) as of 13 September. The Regional Specialized Meteorological Center (RSMC) Tokyo best track data (<https://www.jma.go.jp/jma/jma-eng/jma-center/rsmc-hp-pub-eg/besttrack.html>) is used to validate the results of numerical simulations.

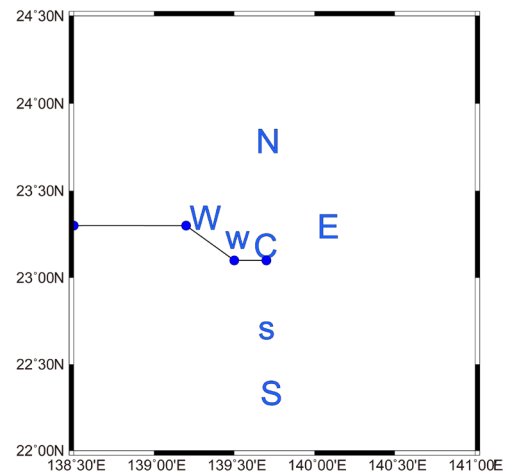


Figure 1 A solid line with closed circles indicates the RSMC-Tokyo best-track locations every 6 hours from 18UTC on 14 to 12 UTC on 15 September. The meaning of alphabets in the panel is explained in the text.

Figure 1 shows the locations of minimum central pressure in each experiment. The character ‘C’ shows the control run. The character ‘N’ means that the atmospheric data at the initial time is shifted northward. The ‘E’, ‘W’ and ‘S’ shows the same meaning as ‘N’ except the direction and distance of the shift. The small characters ‘w’ and ‘s’ are almost the same as ‘W’ and ‘S’ except that the distance of the shift is relatively short. These changes are realized by the modification of Gaussian grid information in the global objective atmospheric analysis data.

3. Results

3.1 Simulated tracks

Figure 2 shows the simulated tracks with the simulated central pressures in all experiments (Fig. 1) simulated by the NHM (Fig. 2a) and CPL (Fig. 2b) with the RSMC-Tokyo best track position with the best-track central pressure. All the simulations tend to show eastward biases after the simulated typhoon passed west of 134°E and north of 26°N compared with the best track. In particular, the eastward biases do increase when the CPL is used instead of the NHM. When shifting the typhoon position south (s or S in Fig. 1) or west (w or W in Fig. 1) at the initial time, the simulated tracks more approach the RSMC best track than that in the other experiments. However, it still fails to simulated the best-track north-westward traveling east of 134°E.

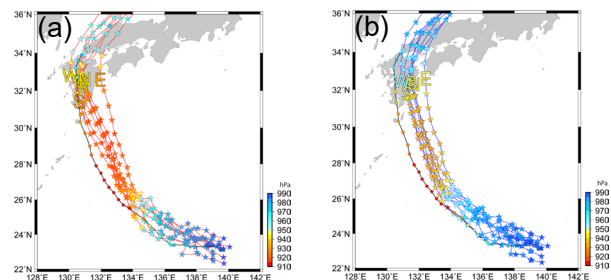


Figure 2 Best track positions every 6 hours with colors indicating the value of best-track central pressures. (a) tracks simulated by the NHM and (b) tracks simulated by the CPL. The alphabets (see Section 2) indicate the location of simulated typhoon at 78 h.

3.2 Simulated central pressures

Figure 3 shows the time series of best track central pressures with individual and ensemble mean central pressures simulated by the NHM and CPL. Central pressures simulated by the NHM tend to be relatively low compared with those simulated by the CPL. The result indicates that ocean coupling helps weaken the intensity of the simulated typhoon irrespective of a different location of the typhoon vortex at the initial time (Fig. 1).

The order of simulated central pressure values among seven numerical experiments at a certain integration time differs between NHM and CPL. The experiment W, which shows the most rapidly deepening and the lowest central pressure in the NHM experiment, does not show such characteristics in the CPL experiment. However, systematic differences in the simulated central pressure between the NHM and CPL experiments may be attributed to the systematic track errors shown in Fig. 2.

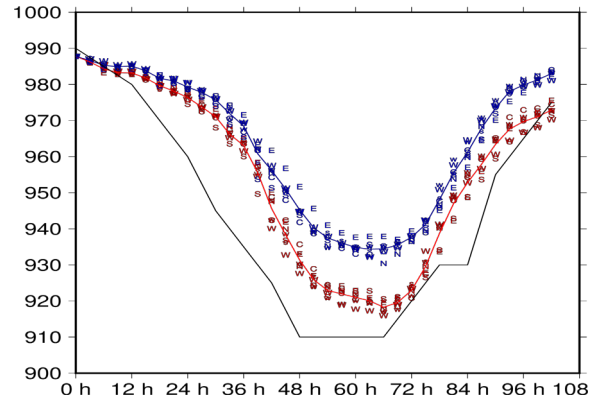


Figure 3 A black solid line indicates the time series of best-track central pressures every 6 hours. Red and blue solid lines indicate the time series of ensemble mean central pressures every 3 hours simulated by the NHM and CPL. The alphabets indicate the result of individual experiment described in Section 2.

3.3 Simulated sea surface temperatures

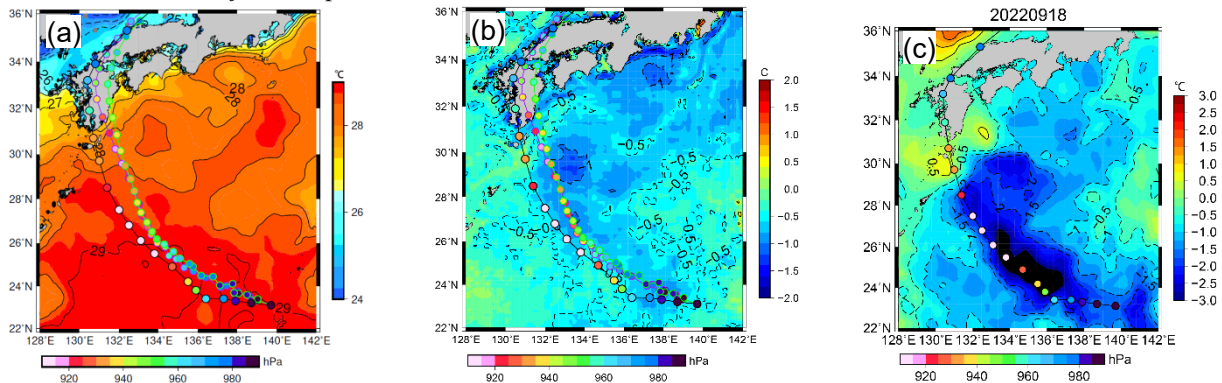


Figure 4 (a) Horizontal distribution of ensemble mean sea surface temperature at 78 h simulated by the CPL with the RSMC best track and tracks by the NHM (purple line) and CPL (green line). (b) Horizontal distribution of the difference in simulated ensemble mean sea surface temperature at 78 h between the NHM and CPL experiments. (c) Horizontal distribution of the variation in microwave optically interpolated sea surface temperature (obtained from <https://www.remss.com/measurements/sea-surface-temperature/>) on 18 September from the sea surface temperature on 13 September. In all panels, colors within the circles indicate the value of central pressure.

Figure 4 shows the horizontal distribution in ensemble mean sea surface temperature at 78 h simulated by the CPL. Sea surface temperature underneath the typhoon does not affect the systematic track errors south of 26°N during the intensification phase since the value of sea surface temperature is higher than 28°C (Fig. 4a) and sea surface cooling along the track is relatively small (Fig. 4b). Simulated decreases in simulated sea surface temperature is remarkable around 29°N , 134°E (Fig. 4b) but decreases in microwave optically interpolated sea surface temperature do appear along the best track even south of 26°N and the magnitude of sea surface cooling is greater than that of simulated sea surface cooling (Fig. 4c). The failure to realistically simulate the minimum sea-level pressure of Nanmadol in the NHM experiments (Fig. 3) may have affected the simulations of track (Fig. 1) and sea surface temperature (Fig. 4a and 4b) in the CPL experiment.

4. Concluding remarks

We show that the simulated track error of Nanmadol may be reduced by changing in the initial position of the typhoon to some extent (within 1 degree) by shifting the atmospheric initial condition. However, it is also clear that this shifting method and ocean coupling does not necessarily improve the systematic track error of Nanmadol west of 134°E . To improve simulated sea surface temperature, realistic simulations on both the intensification rate and the maximum intensity of Nanmadol are required. The improvement of intensity simulations could lead to that of track simulations although the mechanism is not discussed in this report.

It should be noted that the results shown in this study may be different when the other atmosphere-ocean coupled model is used. In addition, the effect of microphysics in the atmosphere model on the track, intensity, and wind rainfall and wind distributions of a typhoon should be explored in the future.

References

Wada, A., S. Kanada, and H. Yamada, 2018: Effect of air–sea environmental conditions and interfacial processes on extremely intense typhoon Haiyan (2013). *Journal of Geophysical Research: Atmospheres*, 123, 10379–10405, <https://doi.org/10.1029/2017JD028139>.